Tumor-activated Neutrophils Promote Metastasis in Breast Cancer via the G-CSF-RLN2-MMP-9 Axis

Youjing Sheng
The First Affiliated Hospital of Anhui Medical University
Weidong Peng
The First Affiliated Hospital of Anhui Medical University
Yan Huang
Anhui Medical University
Lanqing Cheng
the Second Affiliated Hospital of Anhui Medical University
Ye Meng
the Second Affiliated Hospital of Anhui Medical University
Louis Boafo Kwantwi
The First Affiliated Hospital of Anhui Medical University
Jiezhen Yang
Anhui Medical University
Jiegou Xu
Anhui Medical University
Han Xiao
The First Affiliated Hospital of Anhui Medical University
Julia Kzhyshkowska
University of Heidelberg
Qiang Wu (aydjohn@yahoo.com)
The First Affiliated Hospital of Anhui Medical University

Research Article

Keywords: Tumor-associated neutrophils, Breast cancer, NFκB pathway, migration, PI3K-AKT pathway

Posted Date: March 2nd, 2022

DOI: https://doi.org/10.21203/rs.3.rs-1358848/v2

Abstract

Immune component of tumor microenvironment is essential for the regulation of cancer progression. Tumor mass is frequently infiltrated by neutrophils (tumor-associated neutrophils, TANs) in breast cancer (BC) patients. However, the role of TANs and the mechanisms of their action in BC are still unclear. Using quantitative IHC, ROC and Cox analysis, we demonstrate here that high density of TANs infiltrating tumor parenchyma is predictive for poor prognosis and for the decreased progression-free survival of patients with BC that underwent surgical tumor removal without previous neoadjuvant chemotherapy in all 3 cohorts (training cohort, n = 170; validation cohorts, n = 130, independent cohorts, n = 95). Conditioned medium of human breast cancer cell lines prolonged life span of healthy donor neutrophils ex vivo. Neutrophils, activated by supernatants of breast cancer lines, demonstrated the increased ability to stimulate proliferation, migration and invasive activity of breast cancer cells. Cytokines involved in this process have been identified by antibody array. Relationships between these cytokines and density of TANs were validated by ELISA and IHC in fresh breast cancer surgical samples. Identified by antibody arrays, tumor-derived G-CSF significantly prolonged the lifespan and increased the metastasis-promoting activities of neutrophils via PI3K-AKT and NFκB pathway. Simultaneously, TAN-derived RLN2 promoted the migratory abilities of MCF-7 cells via PI3K-AKT-MMP-9. Analysis of tumor tissues from 20 BC patients and RNA-seq from TCGA BC patients identified a positive correlation of density of TANs with the activation of G-CSF-RLN2-MMP-9 axis. Our data indicate that TANs in human breast cancer have detrimental activity supporting malignant cells invasion and migration.

Introduction

Breast cancer is the most commonly diagnosed malignancy among women. Due to advances in early diagnosis and comprehensive treatment, the prognosis of breast cancer patients has improved, which the 5- year overall survival in breast cancer cases to 90% [1, 2]. However, the occurrence rate of metastasis is also increased. Recent studies had shown that 30% of breast cancer patients will develop metastases after surgical treatment which is a contributing factor of cancer related deaths among women [2–4]. Therefore, exploration of the potential mark in predicting breast cancer metastasis and its underlying mechanisms is particularly important.

Neutrophils act as the body's first line of defense against infection and respond to diverse inflammatory cues [5, 6]. In tumor cell line transplantation models and genetically engineered mouse models of cancer, tumor-associated neutrophils (TANs) have been reported to be a component of tumor-promoting inflammation [5–7]. However, neutrophils can engage in pathways of antitumor resistance by killing tumor cells and/or by interacting with other components of immunity [8]. In gastric cancer, TANs have been shown to foster immune suppression and disease progression via GM-CSF-PD-L1 pathway [9]. Additionally, Zhou *et al*. found that TANs increase stem cell characteristics by secreting BMP2 and TGF-β and triggering miR-301-3p expression in hepatocellular carcinoma cells [10]. However, in early stage of lung cancer, TANs inhibit cancer progression by activation T cells response [11]. Therefore the role of TANs in cancer progression remains to be controversial, and can be specific for each type of malignancy.

In this study, we investigated the prognostic value of CD66b + neutrophils density in BC tissues and their correlation with clinical characteristic. Ex vivo, the ability of TANs to promote primary cancer growth and metastatic potential of malignant cells was examined. The signaling pathways that medicate cancer – promoting activity of TANs were identified.

Materials And Methods

Tumor cell culture

MDA-MB-231 and MCF-7 cell lines were provided by the Cell Bank of the Chinese Academy of Sciences. MDA-MB-231 cells were cultured in L15 (HyClone, USA) supplemented with 10% FBS (Gibco, USA) and 100 U/mL penicillin/streptomycin (HyClone).

MCF-7 cells were cultured in MEM (HyClone) supplemented with 10% FBS (Gibco, USA), 100 U/mL penicillin/streptomycin (HyClone) and 0.01 μg/mL insulin.

For the supernatant collected, after the cells adhered, the medium was replaced with SFM (Lonza, Switzerland), and after 72 hours, the supernatants were collected (MDA231CS).

Patient characteristics, IHC and tumor tissue

Formalin-fixed and paraffin-embedded (FFPE) surgical specimens were randomly selected from the First Affiliated Hospital of Anhui Medical University. The samples consisted of equal quantities for each subtype of patients who underwent surgical operations from 2015 to 2016. All these 300 samples were randomly separated into training (n = 170) and validation (n = 130) cohorts. The independent cohort consisted of 95 breast cancer patients FFPE tissues from the Second Affiliated Hospital of Anhui Medical University (Table S1). The last follow-up time was February 10, 2020. All patient were undergoing the treatment followed by CSCO guidance. This study was approved by the Clinical Research Ethics Committee of Anhui Medical University (20180096; 20200976). All procedures performed in this study were in accordance with the ethical standards of the institutional research committee and the 1964 Helsinki Declaration and its later amendments or comparable ethical standards.

Each tumor sample was cut into 2 μm section and used for IHC staining. Antigen retrieval was performed using a pressure cooker for 1.5 minutes in antigen unmasking solution (sodium citrate, pH 6.0). Afterward, samples were incubated with the primary antibody human CD66b (1:100; Cat. 555724.; BD Pharmingen, US) overnight at 4°C and blocked with a biotin block kit (MXB biotechnologies, China) for 20 minutes at room temperature. This was followed by incubation with a secondary antibody (HRP rabbit/mouse Max Vision Kits, MXB biotechnologies) for 20 minutes at room temperature. Then immunodetection was performed by using DAB (MXB biotechnologies) for 3 minutes. Images were obtained by microscopy. After counting the number of neutrophils in 10 HPF, the median was selected as the criterion for dividing the density of TANs into 2 groups.

Neutrophil isolation and treatment

Fresh blood, donated by a healthy volunteer, was treated with EDTA and transferred to a new tube. Following magnetic labeling cells (MACSxpress Neutrophil Isolation Kit, Cat. 130-104-434; Miltenyi; Germany), the tube was put into MACSmix Rotator (Miltenyi) at 37°C for 15 minutes, and neutrophils were suspended in the supernatant. After eliminating erythrocytes with RBC lysing buffer (Cat. 555899; BD Pharmingen; USA), neutrophils were isolated.

Isolated neutrophils were cultured in 6-well culture plates (Corning) with half of MDA231CS and half of serum-free medium or only serum-free medium. For cytokine proving, neutrophils were stimulated with G-CSF (2

ng/ml), CXCL-1 (1.8 ng/ml), GDF-15 (1.4 ng/ml) and PDGF-AA (1 ng/ml) (Peprotech, US) together. To validate the functions G-CSF, we used TANCS combined with neutralized antibody (1.6 mg/ml) (R&D) to -treat neutrophils. To evaluate the signaling pathway, neutrophils were treated with TANCS in the presence of MK2206 (65 nM) or/or JSH-23 (7.1 μM) (Med Chem Express, USA).

Proliferation assays

The assay was performed in 96-well plates. A total of 3×10^3 cancer cells were seeded in each well, and the culture medium was replaced with TANCS, NeuCS, SFM and MDA231CS the next day. After 24 hours, each well was incubated with 10 μl Cell Counting Kits 8 (CCK-8, Bestbio, China) solution at 37°C for 2 hours. The absorbance was measured at 460 nm using a plate reader.

Flow cytometry

The viability of TANs and neutrophils were determined by annexin-V/PI apoptosis detection kits (Biobest). After 10 hours of treatment, TANs and neutrophils were centrifuged at 300 g. After discarding the supernatants, the cells were resuspended in 400 μl Annexin V binding buffer. After incubation with Annexin V-FITC at 4°C for 15 minutes and PI-PE incubation at 4°C for 5 minutes. The data were analyzed by Flowjo (Version. 7.6.1).

Invasion and migration assay

After cancer cells were pretreated with SFM for 12 hours, experiments were performed in an 8 μm-cell culture insert (Corning Company). For the invasion assay, Matrigel (BD Company) diluted with SFM in a 1:8 ratio was precoated in a chamber and solidified for over 2 hours at 37°C. A total of 4×10^4 breast cancer cells suspended in SFM were added to the upper chamber, whereas TANCS or NeuCS were added to the lower chambers. The cancer cells migrated and invaded for both 6 hours. Afterward, cancer cells in the upper chamber were removed with a swab, and the cells attached to the underside of the chambers were fixed with 4% paraformaldehyde for 15 minutes and then stained with 0.5% crystal violet for 1 minute. Quantification was performed by the mean number of cells in five 200x microscopic fields per chamber. In some experiments, in the lower chamber, NeuCS with IL-1γ (2 ng/ml), M-CSF (1.5 ng/ml), MIF (2 ng/ml), RLN2 (1 ng/ml), VEGF (10 ng/ml) and CD31 (3 ng/ml) (Preprotein).

Western Blotting

Protein was extracted with the Nuclear and Cytoplasmic Extraction Kit (Bestbio). For the phosphorylation protein analysis, all lysates were added with phosphatase inhibitor cocktail (MCE). Proteins was loaded onto SDS polyacrylamide gels and then transferred to PVDF membranes. The membranes were blocked 5% BSA in TBST at room temperature for 1 hour. Afterwards, the membranes were incubated with primary antibodies against: anti p-AKT (1:1000; Cat. 4060T; CST, USA), anti-p-STAT3 (1:1000; Cat. 4074S; CST, USA), p-ERK (1:1000; Cat. 4370T; CST, USA), PI3K (1:1000; Cat. 4249S; CST, USA), P65 (1:1000; Cat. 3031S; CST, USA), β-catenin (1:1000; Cat. 4970T; CST, USA), MMP-9 (1:1000; Cat. 13667T; CST, USA), GAPDH (1:1000; Cat. 5174S; CST, USA) and histone H3 (1:1000; Cat. 4499T; CST, USA) at 4°C overnight. Membranes were incubated with Peroxidase-conjugated secondary antibodies (CST) were used, and the antigen-antibody reaction was visualized by enhanced chemiluminescence assay (ECL, Thermo). The signals, as relative units of each lane color density, were evaluated by ImageJ software.

ELISA

Tissue homogenates were isolated from fresh invasive ductal carcinoma samples obtained during surgery. Briefly, 0.1 g tissues were washed with cold normal saline. After removing blood and suspending cold normal saline at a ratio of 1:9, tissues were grinded with a homogenizer at 4° C at 70 rpm for 10 minutes. The samples were centrifuged at 3000 rpm at 4° C, and the supernatants were harvested as the 10% tissue homogenates. G-CSF (Cat. ksk11017, Bioss, China) and RLN2 (Cat. ab243688, Abcam) ELISA kits were purchased from Bioss or Abcam. All experiments were performed according to the manufacturer's instructions.

Immunofluorescent staining

Frozen sections of breast cancer surgical tissues were obtained from the First Affiliated Hospital of Anhui Medical University (20180096; 20200976) and immediately fixed with cold acetone for 15 minutes. This was followed by blocking 1% BSA and 22.52 mg/ml glycine in PBS at room temperature for 1 hour. Sections were co-incubated with combinations of primary antibodies: CD66b (anti- mouse, 1:200; Cat. 555724.; BD Pharmingen, US) and p-AKT (anti- rabbit; 1:400, Cat. 4060T; CST, USA); or CD66b (anti mouse 1:200; Cat. 555724.; BD Pharmingen, US) and p65 (anti- rabbit;1:400, Cat. 3031S; CST, USA). Incubation with primary antibodies was at 4° C overnight. Alexa Goat Anti-Rabbit IgG H&L (Alexa Fluor® 488; 1:10000, Cat. ab150077; Abcam, USA) and Goat Anti-Mouse IgG H&L (Alexa Fluor® 647, 1:10000, Cat. ab150115; Abcam, USA) were used for 1 hour at room temperature in dark places. DAPI was used to counterstain the nuclei. The images were obtained by laser scanning confocal microscopy.

RNA infection

To knock down specific target genes, cells were plated at 5×10^5 cells/mL and transfected with specific siRNA duplexes using Lipofectamine 3000 Transfection Reagent (Invitrogen, catalog no. L3000015) according to the manufacturer's instructions. siRNAs were provided by GenePharma Inc for 3 paired primers and selected due to the PCR (China, Table S3).

Cytokine Antibody Arrays

To evaluate cytokine profiles, cytokine antibody arrays (R&D) were used. TANCS, NeuCS, MDA231CS and SFM were collected and diluted with array buffer. After blocking with array buffer for 1 hour, the array membrane was incubated with 1.5 ml dilution overnight at 4°C. After incubation with HRP-conjugated detection antibodies for 1 hour, outcomes were visualized by ECL (Thermo Fisher). The signals, as relative units of spot color density, were evaluated by ImageJ software.

Biomathematics analyze

The RNA-seq and clinical features data of breast invasive ductal carcinoma were download from (http://www.cbioportal.org/study/summary?id=brca_metabric). After excluding patients without ER statues, PR statues, HER2 statues, lymph nodes involvements, metastasis, stage, progression state and survival time messages, a total 1222 breast cancer RNA- seq were included. Data was analyzed by Perl (Version 5.30.2) and R software (Version 4.1.1). Levels of neutrophils in each breast cancer were calculated by "cibersort" R package [12]. Multi-cox test was analyzed by "survival" and "survminer" R package.

Statistics

Statistical analysis was performed using Prism (version 8.0.1; GraphPad Software) as follows: paired 2-tailed Student's t test (Fig. 2A, B, C and D; Fig. 3, B, C, D and E; Fig. 4B, C and D; Fig. 5A and B; Fig. 5A and B, Fig. 7B

and C, Sig. 5). Multiple and universal COX test (Fig. 1D, G, J, M, Table 1), For all analyses performed, significance was defined as $P < 0.05$.

Table 1
Univariate analysis

	training cohorts			validataion cohorts			independent cohorts		
	HR	95%CI	*P* value	HR	95%CI	*P* value	HR	95%CI	*P* value
high density of TANs	3.07	(2.017,4.685)	0.00	3.77	(2.111,6.73)	0.00	3.02	(1.545,5.888)	0.00
HER2(+)	1.89	(1.206,2.971)	0.01	0.95	(0.403,2.235)	0.90	0.92	(0.444,1.92)	0.83
ER(+)	0.84	(0.561,1.266)	0.41	1.62	(0.875,2.991)	0.13	0.59	(0.301,1.142)	0.12
PR(+)	0.90	(0.594,1.357)	0.61	2.27	(1.177,4.38)	0.01	0.56	(0.286,1.098)	0.09
age < 50	1.06	(0.714,1.584)	0.76	1.08	(0.609,1.926)	0.79	1.01	(0.519,1.964)	0.98
ki-67 > = 30%	1.47	(0.972,2.228)	0.07	0.95	(0.528,1.713)	0.87	1.53	(0.748,3.12)	0.25
LN(+)	1.99	(1.314,3.025)	0.00	1.00	(0.557,1.778)	0.99	1.56	(0.803,3.033)	0.19
stage 3	2.01	(1.316,3.084)	0.00	1.79	(0.643,5)	0.26	3.55	(1.81,6.944)	0.00
T > = 3cm	1.30	(0.846,1.988	0.23	1.00	(0.557,1.778	0.99	3.30	(1.552,7.034	0.00

Results

The high density of TANs was related to the poor prognosis of breast cancer patients.

To investigate the presence of TANs in breast cancer, clinical breast cancer surgical samples (table S1) were obtained from the two institutions and IHC was performed for CD66b. $CD66b^+$ neutrophils infiltrating in the parenchyma of breast cancer tissue counted (Fig. 1A). Median value of the density of TANs was chosen to be the cut-off value to divided into 2 groups.

The prognostic value was then analyzed by survival and Cox multivariate analysis. In all 3 cohorts, high density of TANs was positively correlated to poor PFS for BC patients (training cohort: Fig. 1B, $P < 0.0001$; validation cohort: Fig. 1E, $P < 0.0001$; independent cohort: Fig. 1H, $P = 0.0221 < 0.05$). The univariate analysis showed significant positive association between TANs and PFS in all three cohorts (Table 1). Cox multivariate analysis found that high density of TANs was an independent prognostic factor for poor PFS in all 3 cohorts (training cohort: Fig. 1D, Hazard ratio (HR) = 2.8, $P < 0.001$; validation cohort: Fig. 1G, HR = 4.0, $P < 0.001$; independent cohort: Fig. 1G, HR = 3.5, $P < 0.001$).

The prognostic value TANs were then assessed by ROC analysis. TANs showed a high prognostic value in predicting poor PFS in all training [Fig. 1C, Area under the curve (AUC) = 0.80, 95% confidence interval (CI): 0.74–0.87)], validation (Fig. 1I, AUC = 0.72, 95% CI: 0.75–0.90) and independent (Fig. 1F, AUC = 0.82, 95% CI: 0.61–

0.82) cohorts. The prognostic value of TANs for overall survival were then validation in TCGA datasets. According to the TIMER, high density of TANs was positively correlated to poor OS (Fig. 1K, P = 0.018, HR = 1.36).

To further confirm our findings, 1222 breast cancer patients RNA-seqs from Metabric were downloaded and analyzed. High level of TANs positively related to poor PFS (Fig. 1G, P = 0.023 < 0.05). The univariate analysis found high level of TANs to be associated with worse PFS (*P* = 0.023, HR = 1.29, Supplementary table S2). Cox multivariate analysis also demonstrated that high level of neutrophils was an independent prognostic factor (Fig. 1M, P = 0.018, HR = 1.3).

Activated by BC cells, TANs promoted MCF-7 activities

Neutrophils were isolated from peripheral blood from healthy donates as reported previously[13]. The purity of neutrophils isolated was more than 90% (Fig. S1). Compared with unstimulated neutrophils, a significant increase in the lifespan of neutrophils treated with either MCF7CS (MCF7TANs, *P* = 0.0111) or MDA231CS (MDA231TANs, *P* = 0.0003) was evident. However, the lifespan of MDA231-TANs was significantly higher than that of MCF7TANs (Fig. 2A).

We further evaluated the role of TANs on breast cancer cells. After culturing breast cancer cells with supernatant from either MDA231TANCS and or MCF7TANCS, there was no significantly change was found in the migration and invasion of both MDA-MB-231 and MCF-7 cells respectively (Fig S2). However, MDA231TANCS was found to promote the proliferation (Fig. 2B, P < 0.0001), migration (Fig. 2C, P = 0.0043) and invasion (Fig. 2D, P = 0.0011) abilities of MCF-7 cells (Fig. 2B, 2C, 2D), hence MDA231TANCS was chosen for further investigations.

Neutrophils were activated by tumor-derived G-CSF and turned to TANs in breast cancer

Based on the above findings, the effective components of MDA231CS were then investigated by cytokine antibody arrays. Compared to MDA231CS, the level of G-CSF, CXCL1, GDF-15, and PDGF-AA was significantly lower in TANCS (Fig. 3A).

With all 4 solute mediators, both viability and pro-invasive abilities of TANs were promoted. To identify the most key component, neutrophils were then stimulated by 3 of these 4 cytokines in turn. As results suggested, without rh-G-CSF stimulation, both viability and migration- promotion ability of neutrophils will not be promoted (Fig. 3B, 3C, Fig S3, Fig S4). To further investigate the role of G-CSF, neutrophils were then stimulated by rh-G-CSF. As the result indicated, its viability and abilities of pro-invasive and pro-metastasis were significantly promoted. (Fig. 3B, 3C).

To confirm the role of G-CSF being the main component in activating neutrophils, G-CSF vector was transfected into MCF-7 cells ($GCSF_{high}$- MCF7) to up-regulate its expression of G-CSF. After the exposure to $GCSF_{high}$- MCF7 supernatant, the viability of neutrophils was significantly enhanced. Significantly increased invasion and migration of MCF-7 cells were then observed after the cancer cells were cultured in the supernatant of $GCSF_{high}$- MCF7- TANs (Fig. 3D, 3E).

The relationships between G-CSF and TANs were then investigated in breast cancer surgical tissue. 20 fresh breast cancer tissues and their FFPS tissue were collected. The level of G-CSF was investigated by ELISA, and the density of TANs was evaluated by IHC. The results showed a positive correlation between these two factors (Fig. 3F, P = 0.012, r_s=0.553), which was also demonstrated in breast cancer RNA-seq from TCGA (Fig. 3G, P < 0.0001, r_s=0.156).

PI3K-AKT and NF□B signaling pathway were activated in TANs by G-CSF

The underlying mechanism mediating G-CSF action on neutrophil activation was investigated. Several signaling pathways such as PI3K- AKT, JAK- STAT3, MAPK - ERK1, NFκB and Wnt- β-catenin have been shown to regulate the action of G-CSF on the activation of neutrophils. [14–18]. Compared with neutrophils, levels of PI3K, p-AKT and nuclei- NFκB in TANs and GCSF-TANs were significantly increased. (Fig. 4A, Fig. S5).

After exposure to the MK2206 (AKT inhibitor), the lifespan of TANs was significantly decrease, while the ability to promote tumor activities was not affected. In contrast, after exposing to the JSH-23 (NFκB inhibitor), the ability to promote tumor activities of TANs was a significant decrease, while the lifespan was not affected. Exposure to both inhibitors, neutrophils cannot be activated to TANs by both MDA231CS and rh-G-CSF (Fig. 4B, 4C).

The roles of PI3K-AKT and NFκB were further confirmed in female breast ca ncer tissues by using IF assay. The results showed positive staining signals of p-AKT (Fig. 4D) and nuclei-NFκB (Fig. 4E) located in CD66b + neutrophils, which infiltrated in the parenchyma of breast cancer tissue.

TANs promoted the migration and invasion of MCF-7 cells by activating the RLN2-PI3K-AKT-MMP-9 pathway

The role of TANs on breast cancer cells were then investigated. According to the cytokine array assay, there was a significantly increased expression levels of IL-1ra, M-CSF, MIF, RLN2, VEGF and sCD31 in TANCS (Fig. 3A), which were confirmed by ELISA (Fig. 5A).

After stimulated by all these 6 cytokines together with NeuCS, the migration and invasion of MCF-7 were promoted. To identify key components, MCF-7 cells were then stimulated by NeuCS with 5 of these 6 cytokines in turn. As the results showed, without RLN2 stimulation, the invasion and migration of MCF-7 cells cannot be promoted (Fig. 5B, S6). To identify the role of RLN2 in TANCS, MCF-7 cells were then treated with NeuCS + RLN2. Transwell assay showed, both of the migration and invasion of MCF-7 cells were significantly promoted, while treated with rh-RLN2 alone, no promoted migration and invasion were observed (Fig. 6A). As it had been known that RLN2 targeted on RXFP1 on breast cancer cells, its expression in MCF7 were then knocked down by (siR-MCF7). The MCF-7 cells transfected by si-NC was taken as control (siN-MCF7, Fig. 6S). Treated with TANCS and NeuCS + rh-RLN2 respectively, the migration and invasive of siR-MCF7 cells cannot be promoted, while these two supernatants still promoted this behavior for siN-MCF7 (Fig. 6B).

As it had been known that the RLN2 promoted the breast cancer cell migration and invasive by activating the PI3K-AKT-MMP9 signaling pathway [19], the role of RLN2 pathway were studied. Levels of expression for PI3K, p-AKT and MMP9 in siN-MCF7, TAN-siN-MCF7, Neu-siN-MCF7, Neu + rh-RLN2-siN-MCF7 and TAN-siR-MCF7 were

evaluated by WB. As the results showed, levels of PI3K, p-AKT and MMP9, compared to the siN-MCF7 and Neu-siN-MCF7, were significantly increased in TAN-siN-MCF7, Neu + rRLN2hR-siN-MCF7 respectively. Significantly lower levels of PI3K, p-AKT and MMP9 were found in TAN-siR-MCF7 compared to those in TAN-siN-MCF7. After inhibiting AKT in TAN-siN-MCF7 by MK2206, the level of MMP-9 was significantly decreased (Fig. 7A). After knocking down MMP9 in MCF7 cells by siRNA (siM-MCF7), the migration and invasive of the cancer cells were not promoted, regardless of the treatment of TANCS or NeuCS + RLN2 (Fig. 7B).

The relationships of TANs, RLN2 and MMP9 were evaluated in 20 breast cancer surgical tissues by IHC and ELISA. As the result showed, the density of TANs was positively related to the level the expression of RLN2 (r_S= 0.3976, 95%CI: 0.0029–0.6851, P= 0.0490) and MMP9 (r_s =0.4437, 95%CI: 0.0589–0.7137, P= 0.0263). (Fig. 7C).

Discussion

Accumulating evidence is available for the complex composition and cancer-promoting properties of breast cancer tumor immune microenvironment in patients and animal tumor models [20–22]. Although some immune/inflammatory cells have been shown to interact with breast cancer cells, as the body's first line of defense, the role of neutrophils in cancer microenvironment is largely unknown [5, 23].

Due to the limited knowledge about TANs, its markers for IHC staining and prognostic value in BC patients are not fully defined [5, 11, 24, 25]. Myeloperoxidase (MPO), one of the most abundant proteins in neutrophils [26], had been applied as a marker for TANs in some articles and was are reported to be independently associated with a favorable prognosis in both colorectal and breast cancer. However, MPO is known as an enzyme secreted by neutrophil granulocytes as a result of phagocytosis during inflammation. Hence, MPO-expressing neutrophils are inflammation-activated rather than tumor-activated[27], which makes MPO as a maker for TANs in breast cancer requiring for IHC need further evaluation. CD66b, normally expressed only by neutrophils, had been proven to be an effective marker for neutrophils. Due to their, correlation with the progression of several cancers [28–39], it was applied as a marker of TANs in our study. Consistent with these previous findings, our study found a high density of CD66b + TANs infiltrating in in BC tissues parenchyma positively related with PFS in BC patients. According to the ROC and Cox analysis, the density of CD66b + TANs see not only specific, but also accuracy in predicting the poor PFS in BC patients. These results suggested that evaluating the density of TANs in BC tissue by CD66b immunostaining could be an easily accessible method for predicting progression in BC patients.

Although the density of TANs has been proven to be an effective biomarker for predicting BC metastasis and poor clinical outcomes, its role in cancer progression is still not remains unclear. TANs have had been ignored as a group of immune cells in tumor microenvironments due to their short lifespan (4 to 10 hours). As commonly recognized, the lifespan of inflammation-activated neutrophils is enhanced, which can survive for more than 10 hours [40]. Can the lifespan of TANs be enhanced by cancer cells? Recent studies have shown that the viability of neutrophils to be is enhanced in tumor microenvironments to prolonged than previous known[5, 25]. For this reason, it can be regarded as a novel marker for neutrophil activation. However, the activation of neutrophils to TANs and the interplay with tumor cells remain unclear. It is becoming increasingly clear that TANs can promote tumor progression, the role way of of TANs in several solid tumor are conflicting: their affecting on cancer cells seem to be different in different reports [8]. In GC, TANs isolated from fresh surgical tumor tissues have been

shown to promote immunosuppression and EMT process via GM-CSF-PD-L1[9] and IL-17a[36] pathways respectively. Through recruiting macrophages and T-regulatory cells, TANs have been demonstrated that can promote the growth, progression, and resistance to sorafenib in HCC [41]. While TANs have been shown to regulate other immune cells to enhance their tumor promoting functions, others have reported a direct role of TANs on tumor cells with little evidence on how neutrophils are activated to TANs [36, 42–44]. In this study, we found TANs activated by breast cancer cells to promote the proliferation, invasion and migration of MCF-7 cells. These results indicated that, in breast cancer microenvironments, neutrophils activated by breast cancer cells can promote the biological behavior of cancer cells, suggesting an interaction between cancer cells and infiltrating neutrophils.

Accumulating evidence have suggested that cytokines including but not limited to IL8[45], IL6[33], can alter the phenotype of neutrophils towards tumor promoting effects [46]. Herein, we found G-CSF was the key component in MDA231CS prolonging the lifespan and metastasis abilities of TANs. Our study on breast cancer tissues and surgical tissues also showed a positive correlation between TANs and the expression of G-CSF. It is known that G-CSF is a critical regulator of the proliferation, differentiation, and survival of granulocytes [47, 48]. Previous study showed that G-CSF promoted mouse granulocytes, Ly6G cells, differentiation and decreased T cell proliferation and promoted pancreatic ductal adenocarcinoma growth in a mouse model [49]. High levels of G-CSF expression have been observed and reported to be associated with poor OS in human triple-negative BC [24]. However, G-CSF' role in TANs activation in BC were seldomly reported. In mouse models, 4T1 murine mammary tumors are known to produce G-CSF and increase the numbers of immunosuppressive CD11bGr1 myeloid-derived suppressor cells (MDSCs) in tissues such as the spleen and lungs of tumor-bearing mice [50]. Studies in mice also showed that pretreatment with recombinant G-CSF promotes 4T1 cell lung metastasis by modifying Ly6G + Ly6C + granulocytes [51]. The above research supports the results of our study, which showed that tumor-derived G-CSF can activate neutrophils to enhance metastasis of breast cancer cells. However, in this study, both MDA231-TANs and MCF7-TANs cannot promote the invasion and migration of their own breast cancer cell lines which was same as it previous reported [10]. A previous study has demonstrated a high production of G-CSF in MDA-MB-231 cells than in MCF-7 cells to trigger the activation of M2 TAMs [24]. Accordingly, we observed that after the upregulation of G-CSF in MCF-7 cells, MCF7-TANs significantly promoted the migration and invasive of MCF-7 cells. In a mouse model, polarization of neutrophils by G-CSF has been shown to promote pulmonary and lymph node metastases [48]. Taken together, our findings and the aforementioned studies suggest that G-CSF plays an important role in the activation and tumor promoting functions of TANs in breast cancer tumor microenvironments.

Besides Wang's report on activation of neutrophils to induce PD-L1 expression via G-CSF/JAK/STAT-3 cell signaling pathway of PD-L1[9], the signaling pathway regulating TANs activation in breast cancer is unknown. Our study showed the expression of PI3K, p-AKT and nuclei NFκB p65 to be significantly upregulated in TANs. This suggested that the G-CSF-PI3K-AKT signaling pathway activated and prolonged the lifespan of TANs while G-CSF –NFκB pathway regulated the pro-metastatic ability of TANs in breast cancer cells. This finding reveals a new insight into the role of TANs in BC.

Our study showed that the level of RLN2 was significantly increased in TANCS and these TAN-derived RLN2 was the key component which promoted the invasion and migration of BC cells via PI3K-AKT-MMP-9 axis. These results were also proved in BC surgical tissues, where a positive correlation among the density of TANs and the expression of RLN2 and MMP-9 was observed. RLN2 is known to play an important role in pregnancies,

including those of humans. However, its role in cancer still remains very controversial [52]. Studies on endometrial cancer and prostatic carcinoma have proved that RLN2 promotes the metastasis and invasion of cancer cells and could be a biomarker to predict prognosis[53]. In BC, although RLN2 is already known to promote in vitro invasiveness by upregulating MMP-9 expression in BC cell lines, the findings regarding its functions still remain conflicts [54]. Binder *et al.* reported RLN2 serum levels to correlate positively to the metastatic of BC[55]. Others have reported that RLN2 can promote the of breast cancer cells by upregulating S100A/MMP-9 signaling [54, 56]. However, our study is the first to show the presence of RLN2 in TANs-conditioned medium rather than RLN2 alone to promote the migration of BC cells. We also found that by targeting RLN2 receptor, RXFP1, TANs-derived RLN2 promoted the metastasis of BC cells by upregulating the expression of MMP-9 via PI3K-AKT signaling pathway. However, others have reported that RLN2 as a matrix-depleting agent, has the potential to improve penetration and consequently the efficacy of anticancer immunotherapies and chemotherapies [57, 58]. Therefore, targeting the RXFP1-RLN2 pathway appears to have both antitumor and protumor effects. A Study in HCC have demonstrated that the upregulation of RLN2 mitigates liver metastasis [58], while others found that both ligand-derived and receptor antagonists targeting RLN2 and RXFP1 respectively could result in antitumor activities in xenograft models of prostatic cancer[59]. Recently, Sumera *et al.* explained that these two faces of the pathway is largely depended on the delivery method of RLN2 and tumor type[52]. According to our study, RLN2 secreted by TANs promoted the migration of BC cells.

Our study indicated that high density of TANs in BC is positively related to cancer metastasis and poor outcomes, and as proved in vitro, TANs promote the migration and invasion of BC cells via G-CSF-RLN2-MMP-9 axis. CD66b positive TANs in BC tissue could be a useful marker for predicting BC metastasis and PFS. Targeting either RLN2-RXFP1 or G-CSF might provide a new therapeutic strategy for the treatment of metastatic BC.

Declarations

Availability of data and materials

The datasets used and/or analysed during the current study are available from the corresponding author on reasonable request

Conflict of Interest

The authors declare that the research was conducted in the absence of any commercial or financial relationships that could be construed as a potential conflict of interest.

Fundings

Anhui Institute of Translational Medicine2017zhyx36, 2017zhyx36. Special Fund for Discipline Leaders of Anhui Province, 2019H230

Authors' contributions

Qiang Wu and Youjing Sheng designed the experiments; Youjing Sheng performed most of the experiments and compiled and analyzed the data; Youjing Sheng initiated the experimental works. Weidong Peng and Lanqin Cheng contributed to certain key experiments. Youjing Sheng and Ye Meng prepared the figures; Youjing Sheng conducted the mathematical modeling; Jiegou Xu, Han Xiao and Jiezhen Yang were involved in specific experiments; Qiang Wu provided resources and Yan Huang advised on experimental protocols; Youjing Sheng, Louis, Julia Julia Kzhyshkowska and Qiang Wu wrote the manuscript; Qiang Wu funded the work and provided overall research supervision.

Acknowledgments

This work was supported by funds from the National Natural Science Funds Fund. We thank Professors Xu Jiegou for advice on neutrophil isolation. We thank Xiaowen Han, Yongsheng Fang, Yu Xia, Jingbo Fan and Dachao Liu for the donation of blood. We thank the Flow Cytometry Center at the Laboratory Department in the First Affiliated Hospital of Anhui Medical University and the Laser Scanning Confocal Microscopy Center of the Center for Scientific Research of Anhui Medical University.

Study Approval

Tumor resections were obtained from breast cancer patients at First Affiliated Hospital of Anhui Medical University. All cases are untreated primary tumors. Before resection, informed consent was given and the collection of patient samples was approved by the ethical review board of Anhui Medical University Institute (20180096; 20200976) and in accordance with the Declaration of Helsinki. Peripheral blood samples were obtained from 5 healthy volunteers (20200976).

Consent for publication

Not applicable

References

1. Chen W, Zheng R, Baade PD, Zhang S, Zeng H, Bray F, Jemal A, Yu XQ, He J: **Cancer statistics in China, 2015**. *CA Cancer J Clin* 2016, **66**(2):115-132.
2. Siegel RL, Miller KD, Fuchs HE, Jemal A: **Cancer Statistics, 2021**. *CA Cancer J Clin* 2021, **71**(1):7-33.
3. Harbeck N, Penault-Llorca F, Cortes J, Gnant M, Houssami N, Poortmans P, Ruddy K, Tsang J, Cardoso F: **Breast cancer**. *Nat Rev Dis Primers* 2019, **5**(1):66.
4. Liang Y, Zhang H, Song X, Yang Q: **Metastatic heterogeneity of breast cancer: Molecular mechanism and potential therapeutic targets**. *Seminars in cancer biology* 2020, **60**:14-27.
5. Shaul ME, Fridlender ZG: **Tumour-associated neutrophils in patients with cancer**. *Nat Rev Clin Oncol* 2019, **16**(10):601-620.
6. Coffelt SB, Wellenstein MD, de Visser KE: **Neutrophils in cancer: neutral no more**. *Nat Rev Cancer* 2016, **16**(7):431-446.
7. Mantovani A, Cassatella MA, Costantini C, Jaillon S: **Neutrophils in the activation and regulation of innate and adaptive immunity**. *Nat Rev Immunol* 2011, **11**(8):519-531.

8. Jaillon S, Ponzetta A, Di Mitri D, Santoni A, Bonecchi R, Mantovani A: **Neutrophil diversity and plasticity in tumour progression and therapy**. *Nat Rev Cancer* 2020, **20**(9):485-503.
9. TT W, YL Z, LS P, N C, W C, YP L, FY M, JY Z, P C, YS T *et al*: **Tumour-activated neutrophils in gastric cancer foster immune suppression and disease progression through GM-CSF-PD-L1 pathway**. 2017, **66**(11):1900-1911.
10. Zhou SL, Yin D, Hu ZQ, Luo CB, Zhou ZJ, Xin HY, Yang XR, Shi YH, Wang Z, Huang XW *et al*: **A Positive Feedback Loop Between Cancer Stem-Like Cells and Tumor-Associated Neutrophils Controls Hepatocellular Carcinoma Progression**. *Hepatology (Baltimore, Md)* 2019, **70**(4):1214-1230.
11. Eruslanov EB, Bhojnagarwala PS, Quatromoni JG, Stephen TL, Ranganathan A, Deshpande C, Akimova T, Vachani A, Litzky L, Hancock WW *et al*: **Tumor-associated neutrophils stimulate T cell responses in early-stage human lung cancer**. *J Clin Invest* 2014, **124**(12):5466-5480.
12. Newman AM, Liu CL, Green MR, Gentles AJ, Feng W, Xu Y, Hoang CD, Diehn M, Alizadeh AA: **Robust enumeration of cell subsets from tissue expression profiles**. *Nature methods* 2015, **12**(5):453-457.
13. T T, A G, S N-K, B W, T K, Molecular H-KSJ, endocrinology c: **Emerging roles for the relaxin/RXFP1 system in cancer therapy**. 2019, **487**:85-93.
14. Aliper AM, Frieden-Korovkina VP, Buzdin A, Roumiantsev SA, Zhavoronkov A: **A role for G-CSF and GM-CSF in nonmyeloid cancers**. *Cancer medicine* 2014, **3**(4):737-746.
15. Mehta HM, Malandra M, Corey SJ: **G-CSF and GM-CSF in Neutropenia**. *Journal of immunology (Baltimore, Md : 1950)* 2015, **195**(4):1341-1349.
16. Al-Rashed F, Thomas R, Al-Roub A, Al-Mulla F, Ahmad R: **LPS Induces GM-CSF Production by Breast Cancer MDA-MB-231 Cells via Long-Chain Acyl-CoA Synthetase 1**. *Molecules (Basel, Switzerland)* 2020, **25**(20).
17. Akira S, Kishimoto T: **IL-6 and NF-IL6 in acute-phase response and viral infection**. *Immunological reviews* 1992, **127**:25-50.
18. Brasier AR: **Therapeutic targets for inflammation-mediated airway remodeling in chronic lung disease**. *Expert review of respiratory medicine* 2018, **12**(11):931-939.
19. Valkovic AL, Bathgate RA, Samuel CS, Kocan M: **Understanding relaxin signalling at the cellular level**. *Molecular and cellular endocrinology* 2019, **487**:24-33.
20. Vikas P, Borcherding N, Zhang W: **The clinical promise of immunotherapy in triple-negative breast cancer**. *Cancer Manag Res* 2018, **10**:6823-6833.
21. Larionova I, Tuguzbaeva G, Ponomaryova A, Stakheyeva M, Cherdyntseva N, Pavlov V, Choinzonov E, Kzhyshkowska J: **Tumor-Associated Macrophages in Human Breast, Colorectal, Lung, Ovarian and Prostate Cancers**. *Front Oncol* 2020, **10**:566511.
22. Ma RY, Zhang H, Li XF, Zhang CB, Selli C, Tagliavini G, Lam AD, Prost S, Sims AH, Hu HY *et al*: **Monocyte-derived macrophages promote breast cancer bone metastasis outgrowth**. *J Exp Med* 2020, **217**(11).
23. Safarulla S, Madan A, Xing F, Chandrasekaran A: **CXCR2 Mediates Distinct Neutrophil Behavior in Brain Metastatic Breast Tumor**. *Cancers* 2022, **14**(3):515.
24. Hollmén M, Karaman S, Schwager S, Lisibach A, Christiansen AJ, Maksimow M, Varga Z, Jalkanen S, Detmar M: **G-CSF regulates macrophage phenotype and associates with poor overall survival in human triple-negative breast cancer**. *Oncoimmunology* 2016, **5**(3):e1115177.

25. Giese MA, Hind LE, Huttenlocher A: **Neutrophil plasticity in the tumor microenvironment**. *Blood* 2019, **133**(20):2159-2167.
26. Metzler KD, Fuchs TA, Nauseef WM, Reumaux D, Roesler J, Schulze I, Wahn V, Papayannopoulos V, Zychlinsky A: **Myeloperoxidase is required for neutrophil extracellular trap formation: implications for innate immunity**. *Blood* 2011, **117**(3):953-959.
27. KA M, RL A, journal HJJTF: **Neutrophils, G-CSF and their contribution to breast cancer metastasis**. 2018, **285**(4):665-679.
28. Posabella A, Kohn P, Lalos A, Wilhelm A, Mechera R, Soysal S, Muenst S, Guth U, Stadlmann S, Terracciano L *et al*: **High density of CD66b in primary high-grade ovarian cancer independently predicts response to chemotherapy**. *J Cancer Res Clin Oncol* 2020, **146**(1):127-136.
29. Yamada Y, Nakagawa T, Sugihara T, Horiuchi T, Yoshizaki U, Fujimura T, Fukuhara H, Urano T, Takayama K, Inoue S *et al*: **Prognostic value of CD66b positive tumor-infiltrating neutrophils in testicular germ cell tumor**. *BMC Cancer* 2016, **16**(1):898.
30. Rakaee M, Busund LT, Paulsen EE, Richardsen E, Al-Saad S, Andersen S, Donnem T, Bremnes RM, Kilvaer TK: **Prognostic effect of intratumoral neutrophils across histological subtypes of non-small cell lung cancer**. *Oncotarget* 2016, **7**(44):72184-72196.
31. Matsumoto Y, Mabuchi S, Kozasa K, Kuroda H, Sasano T, Yokoi E, Komura N, Sawada K, Kimura T: **The significance of tumor-associated neutrophil density in uterine cervical cancer treated with definitive radiotherapy**. *Gynecol Oncol* 2017, **145**(3):469-475.
32. Kitano Y, Okabe H, Yamashita YI, Nakagawa S, Saito Y, Umezaki N, Tsukamoto M, Yamao T, Yamamura K, Arima K *et al*: **Tumour-infiltrating inflammatory and immune cells in patients with extrahepatic cholangiocarcinoma**. *Br J Cancer* 2018, **118**(2):171-180.
33. Cheng Y, Li H, Deng Y, Tai Y, Zeng K, Zhang Y, Liu W, Zhang Q, Yang Y: **Cancer-associated fibroblasts induce PDL1+ neutrophils through the IL6-STAT3 pathway that foster immune suppression in hepatocellular carcinoma**. *Cell death & disease* 2018, **9**(4):422.
34. Huang X, Pan Y, Ma J, Kang Z, Xu X, Zhu Y, Chen J, Zhang W, Chang W, Zhu J: **Prognostic significance of the infiltration of CD163(+) macrophages combined with CD66b(+) neutrophils in gastric cancer**. *Cancer Med* 2018, **7**(5):1731-1741.
35. Dabrosin N, Sloth Juul K, Baehr Georgsen J, Andrup S, Schmidt H, Steiniche T, Heide Ollegaard T, Bonnelykke Behrndtz L: **Innate immune cell infiltration in melanoma metastases affects survival and is associated with BRAFV600E mutation status**. *Melanoma Res* 2019, **29**(1):30-37.
36. Li S, Cong X, Gao H, Lan X, Li Z, Wang W, Song S, Wang Y, Li C, Zhang H *et al*: **Tumor-associated neutrophils induce EMT by IL-17a to promote migration and invasion in gastric cancer cells**. *Journal of experimental & clinical cancer research : CR* 2019, **38**(1):6.
37. Ye L, Zhang T, Kang Z, Guo G, Sun Y, Lin K, Huang Q, Shi X, Ni Z, Ding N *et al*: **Tumor-Infiltrating Immune Cells Act as a Marker for Prognosis in Colorectal Cancer**. *Front Immunol* 2019, **10**:2368.
38. Shaul ME, Eyal O, Guglietta S, Aloni P, Zlotnik A, Forkosh E, Levy L, Weber LM, Levin Y, Pomerantz A *et al*: **Circulating neutrophil subsets in advanced lung cancer patients exhibit unique immune signature and relate to prognosis**. *FASEB J* 2020, **34**(3):4204-4218.

39. Mandelli GE, Missale F, Bresciani D, Gatta LB, Scapini P, Caveggion E, Roca E, Bugatti M, Monti M, Cristinelli L *et al*: **Tumor Infiltrating Neutrophils Are Enriched in Basal-Type Urothelial Bladder Cancer**. *Cells* 2020, **9**(2).
40. ZG F, Carcinogenesis ASJ: **Tumor-associated neutrophils: friend or foe?** 2012, **33**(5):949-955.
41. SL Z, ZJ Z, ZQ H, XW H, Z W, EB C, J F, Y C, Z D, J Z: **Tumor-Associated Neutrophils Recruit Macrophages and T-Regulatory Cells to Promote Progression of Hepatocellular Carcinoma and Resistance to Sorafenib**. *Gastroenterology* 2016, **150**(7):1646-1658.e1617.
42. Chao T, Furth EE, Vonderheide RH: **CXCR2-Dependent Accumulation of Tumor-Associated Neutrophils Regulates T-cell Immunity in Pancreatic Ductal Adenocarcinoma**. *Cancer Immunol Res* 2016, **4**(11):968-982.
43. Governa V, Trella E, Mele V, Tornillo L, Amicarella F, Cremonesi E, Muraro MG, Xu H, Droeser R, Däster SR *et al*: **The Interplay Between Neutrophils and CD8(+) T Cells Improves Survival in Human Colorectal Cancer**. *Clin Cancer Res* 2017, **23**(14):3847-3858.
44. Wang Y, Chen J, Yang L, Li J, Wu W, Huang M, Lin L, Su S: **Tumor-Contacted Neutrophils Promote Metastasis by a CD90-TIMP-1 Juxtacrine-Paracrine Loop**. *Clin Cancer Res* 2019, **25**(6):1957-1969.
45. Bakouny Z, Choueiri TK: **IL-8 and cancer prognosis on immunotherapy**. *Nature medicine* 2020, **26**(5):650-651.
46. Mukaida N, Sasaki SI, Baba T: **Two-Faced Roles of Tumor-Associated Neutrophils in Cancer Development and Progression**. *International journal of molecular sciences* 2020, **21**(10).
47. Mouchemore KA, Anderson RL, Hamilton JA: **Neutrophils, G-CSF and their contribution to breast cancer metastasis**. *FEBS J* 2018, **285**(4):665-679.
48. Coffelt SB, Kersten K, Doornebal CW, Weiden J, Vrijland K, Hau CS, Verstegen NJM, Ciampricotti M, Hawinkels L, Jonkers J *et al*: **IL-17-producing γδ T cells and neutrophils conspire to promote breast cancer metastasis**. *Nature* 2015, **522**(7556):345-348.
49. Pickup MW, Owens P, Gorska AE, Chytil A, Ye F, Shi C, Weaver VM, Kalluri R, Moses HL, Novitskiy SV: **Development of Aggressive Pancreatic Ductal Adenocarcinomas Depends on Granulocyte Colony Stimulating Factor Secretion in Carcinoma Cells**. *Cancer Immunol Res* 2017, **5**(9):718-729.
50. Bosiljcic M, Cederberg RA, Hamilton MJ, LePard NE, Harbourne BT, Collier JL, Halvorsen EC, Shi R, Franks SE, Kim AY *et al*: **Targeting myeloid-derived suppressor cells in combination with primary mammary tumor resection reduces metastatic growth in the lungs**. *Breast Cancer Res* 2019, **21**(1):103.
51. Kowanetz M, Wu X, Lee J, Tan M, Hagenbeek T, Qu X, Yu L, Ross J, Korsisaari N, Cao T *et al*: **Granulocyte-colony stimulating factor promotes lung metastasis through mobilization of Ly6G+Ly6C+ granulocytes**. *Proceedings of the National Academy of Sciences of the United States of America* 2010, **107**(50):21248-21255.
52. Rizvi S, Gores GJ: **The Two Faces of Relaxin in Cancer: Antitumor or Protumor?** *Hepatology* 2020, **71**(3):1117-1119.
53. Fue M, Miki Y, Takagi K, Hashimoto C, Yaegashi N, Suzuki T, Ito K: **Relaxin 2/RXFP1 Signaling Induces Cell Invasion via the β-Catenin Pathway in Endometrial Cancer**. *Int J Mol Sci* 2018, **19**(8).
54. Cao WH, Liu HM, Liu X, Li JG, Liang J, Liu M, Niu ZH: **Relaxin enhances in-vitro invasiveness of breast cancer cell lines by upregulation of S100A4/MMPs signaling**. *European review for medical and pharmacological sciences* 2013, **17**(5):609-617.

55. Binder C, Simon A, Binder L, Hagemann T, Schulz M, Emons G, Trümper L, Einspanier A: **Elevated concentrations of serum relaxin are associated with metastatic disease in breast cancer patients**. *Breast Cancer Res Treat* 2004, **87**(2):157-166.
56. Binder C, Hagemann T, Husen B, Schulz M, Einspanier A: **Relaxin enhances in-vitro invasiveness of breast cancer cell lines by up-regulation of matrix metalloproteases**. *Molecular human reproduction* 2002, **8**(9):789-796.
57. Hu M, Zhou X, Wang Y, Guan K, Huang L: **Relaxin-FOLFOX-IL-12 triple combination therapy engages memory response and achieves long-term survival in colorectal cancer liver metastasis**. *J Control Release* 2020, **319**:213-221.
58. Hu M, Wang Y, Xu L, An S, Tang Y, Zhou X, Li J, Liu R, Huang L: **Relaxin gene delivery mitigates liver metastasis and synergizes with check point therapy**. *Nat Commun* 2019, **10**(1):2993.
59. Feng S, Agoulnik IU, Truong A, Li Z, Creighton CJ, Kaftanovskaya EM, Pereira R, Han HD, Lopez-Berestein G, Klonisch T *et al*: **Suppression of relaxin receptor RXFP1 decreases prostate cancer growth and metastasis**. *Endocr Relat Cancer* 2010, **17**(4):1021-1033.

Figures

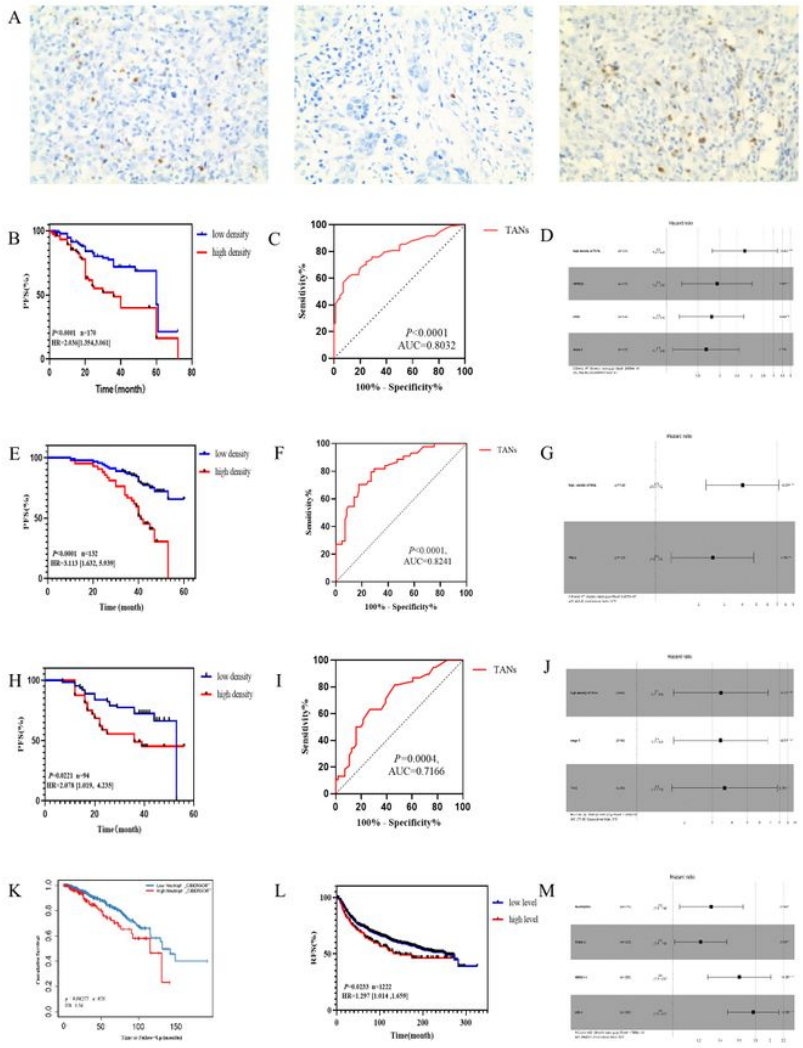

Figure 1

TANs, infiltrating in tumor parenchyma, are associated with poor PFS of breast cancer patients. Representative image for IHC staining of CD66b+ neutrophils were detected in the breast cancer patients' parenchyma tissues. Scale bars, 50 μm(A). Kaplan–Meier survival curves for patients with high and low density of TANs training (n=170), validation (n=129) and independent (n=94), TCGA (n= 838) and Metabric (n =1222) cohorts respectively. The cutoff points for TANs were determined based on median value. High density of TANs was related to poor PFS both training (*P*<0.001, HR= 2.04), validation (*P*=0.03, HR= 2.25) and independent (*P*=0.03, HR= 1.46) cohorts (C, E). ROC analysis and AUC were applied for accessing the prognostic capacity of PFS

according to the TANs. As results showed a high prognostic value of TANs in predicting PFS in both training (AUC =0.80), validation (AUC =0.82) and independent (AUC =0.0.72) cohorts respectively (B, E, H). Multiple Cox test suggested that high density of TANs was the independent risk factor in breast cancer patients' progression of all training (HR =2.8), validation (HR=4.0) and independent (HR=3.4) cohorts (D, G, J and M).

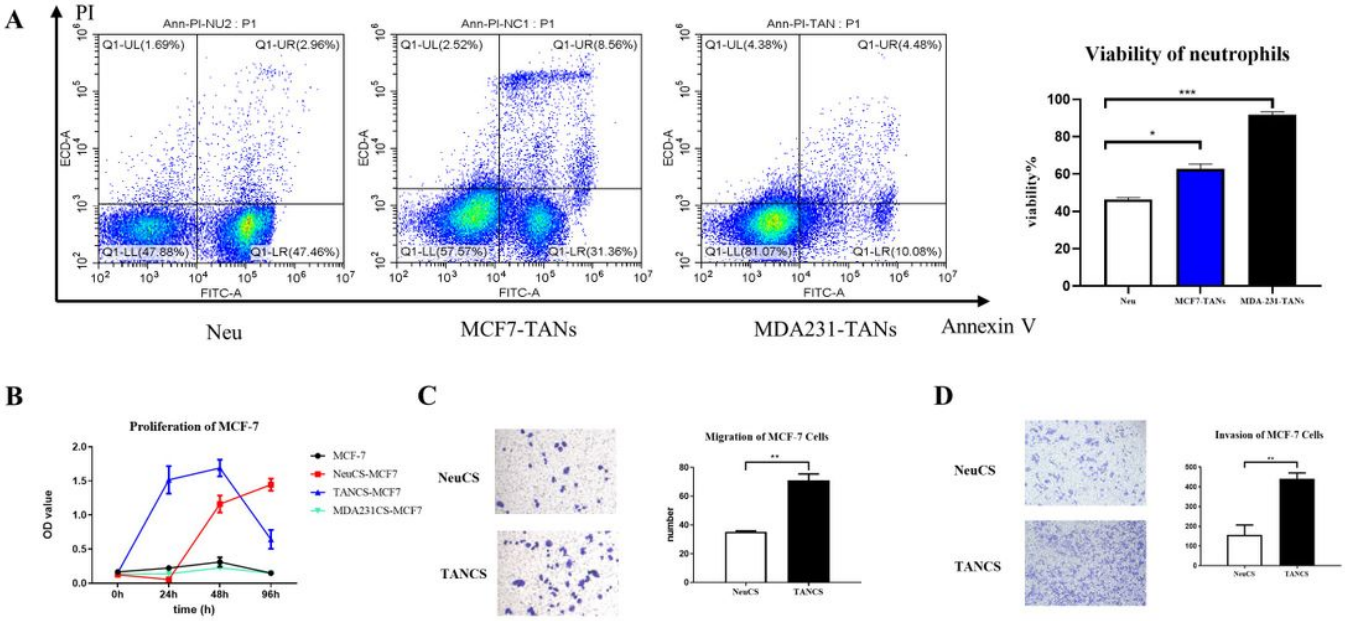

Figure 2

After treated with breast cancer cells cultured supernatant, neutrophils were activated to TANs and promoted biological behavior of breast cancer cell. After treated with MCF7CS or MDA231CS, lifespan of neutrophils was evaluated by flow cytometry. As the result showed, lifespan of MCF-TANs (*P*=0.0111) and MDA231- TANs (*P*=0.0003) were significantly promoted (A,D). After treated with MDA231CS, the proliferation of MCF-7 cells was evaluated by CCK8 in 24h, 48h, 96h separately. The proliferation of MCF-7 was significantly promoted in 24h and 48h (B, D*P*<0.0001). The migration and invasion of MCF-7 cells after treated with MDA231CS by transwell. the resulted showed, migration (C, *P*= 0.0043) and invasion (D, *P*= 0.0011) abilities of MCF-7 cells were significantly promoted. Magnification: x200.

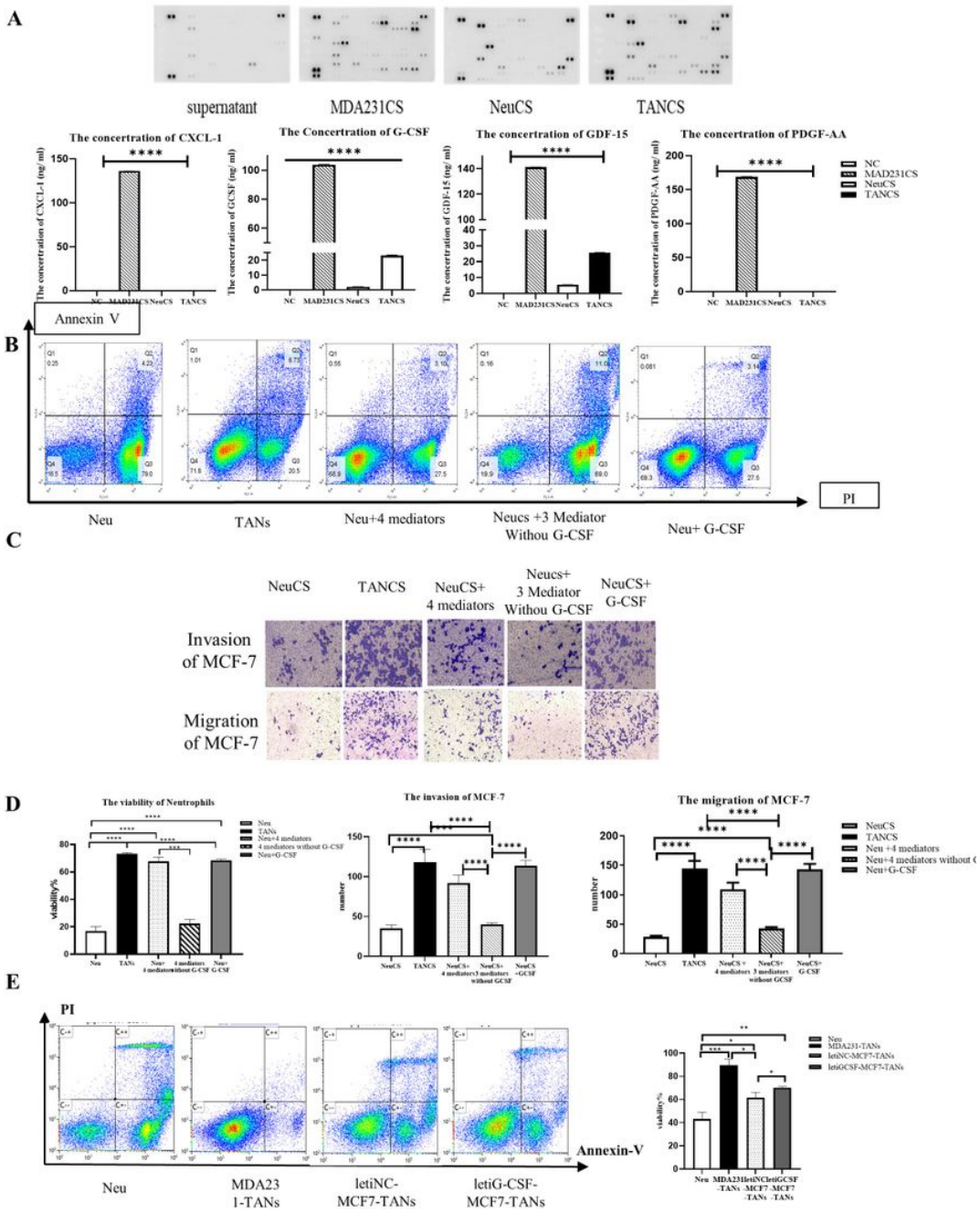

Figure 3

Tumor-derived G-CSF activated neutrophils into TANs in breast cancer. The effective components in MDA231CS for activating TANs was screening by antibody array assay and showed that comparing cells cultured with NeuCS and TANCS, the expression level of G-CSF, CXCL1, GDF-15, and PDGF-AA was expressed at higher levels in cells cultured with TANCS. There were confirmed by ELISA n=3. (A). Viability of neutrophils exposed to four cytokines. The neutrophils were activated by total four cytokines (P<0.0001). When left G-CSF, other 3 cytokines could not promote the viability of neutrophils. Treated neutrophils with G-CSF, the viability of neutrophils was not promoted (P<0.0001). With only G-CSF stimulated, the viability of neutrophils was enhanced (P<0.0001), n=3.

(B,D). Activated by total cytokines, the neutrophils significantly promoted the migration and invasion of MCF-7, while left GCSF, this promotion cannot be seen. Activated by G-CSF, the neutrophils promoted the invasive and migration of MCF-7 cells (C,D). After stimulated neutrophils by leti-G-CSF in MCF-7, the viability of neutrophils promoted (E, *P*= 0.0325),

and it promoted the migration (*P*= 0.0008) and invasion (*P*=0.0014) of MCF-7 compared to letiNC-MCF-7 activated neutrophils. n=3. *, *P* <0.05. **, *P* <0.01. ***, *P* < 0.005 (E). The relationships of G-CSF were positively related to the density of TANs in both breast cancer tissue (F, n= 20, *P*=0.012, r_s=0.553).

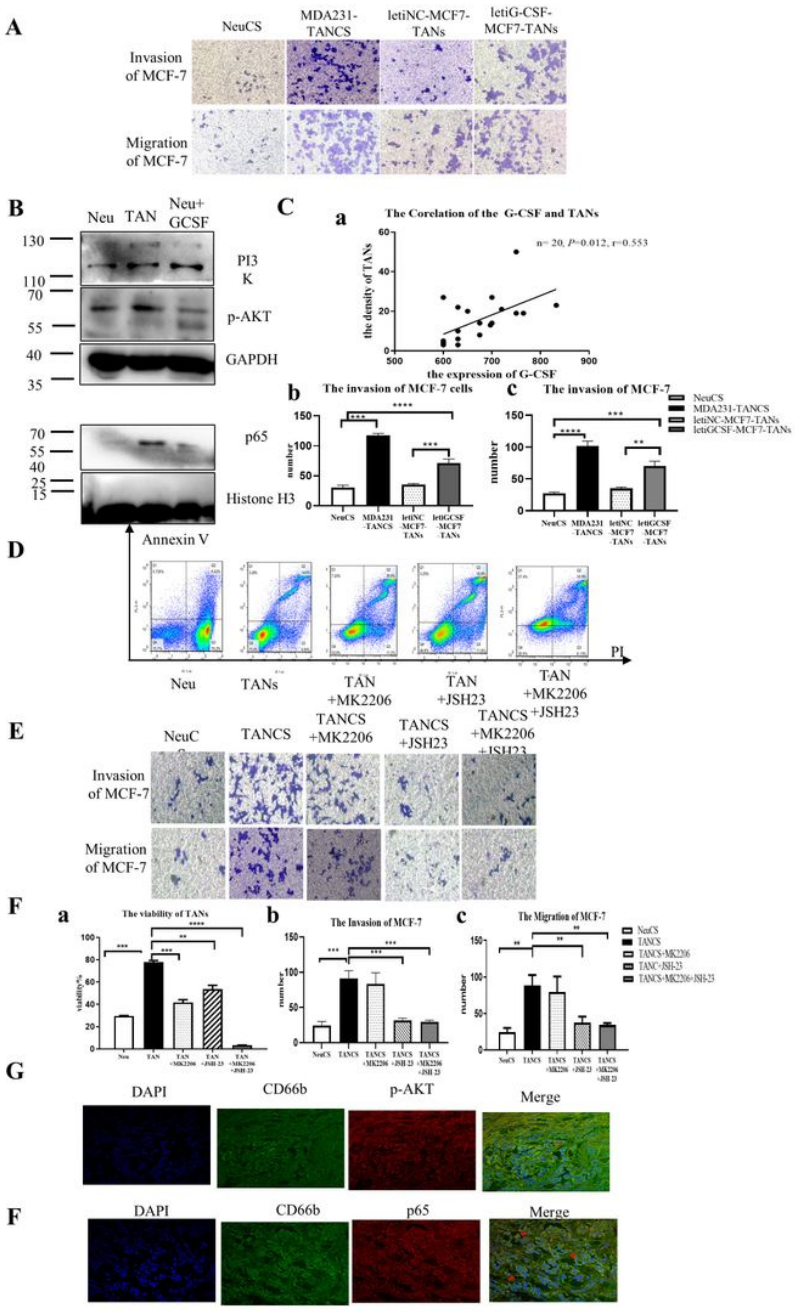

Figure 4

G-CSF activated TANs in breast cancer via PI3K-AKT and NF□B signaling pathway. Leti-GCSF- MCF7- TANs promoted the invasion and migration of MCF-7 (A, Cb, Cd). In breast cancer surgical tissues, the positive correlation of the expression of G-CSF, and the density of TANs were found (C). The expression of PI3K, p-AKT and nuclei-p65 were detected in TANs. Compared to the neutrophils, expression of these were promoted in TANs and GCSF-TANs (B). After inhibited AKT(MK2206), the viability of TANs cannot be promoted (D, Fa), while inhibited NFκb (JSH23), the invasion and migration abilities of TANs cannot be promoted. Inhibited both, the viability and promotion behavior cannot be promoted in TANs (E, Fb, Fc). The TANs marked by CD66b(red) expressed p-AKT (green) (G) and p65 (green) (F).

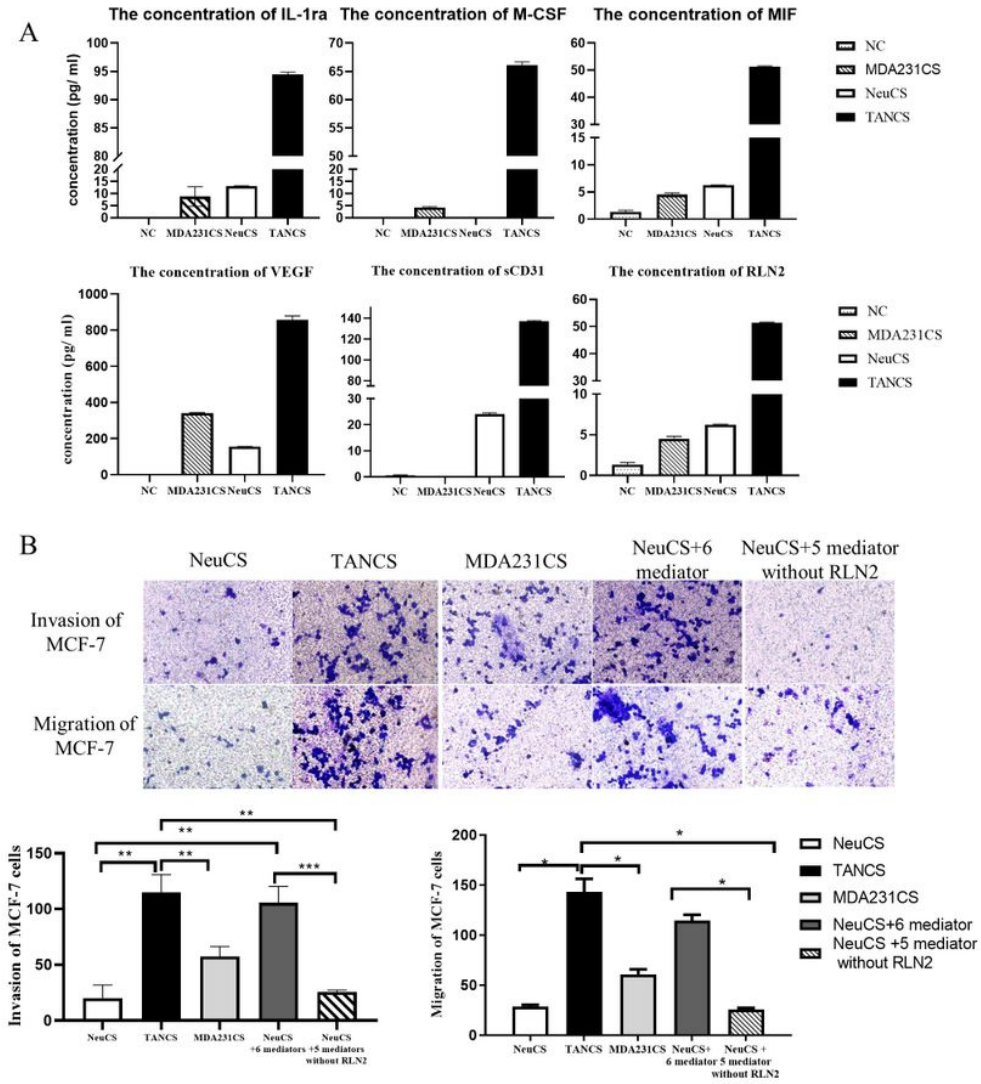

Figure 5

TANs promoted the migration and invasion of MCF-7 cells by activating the RLN2-PI3K-AKT-MMP-9 pathway. ELISA were confirmed the increasing levels of IL-1ra, M-CSF, MIF, RLN2, VEGF and sCD31 in TANCS (A). RLN2 was the key component in TANCS which promoted the invasion and migration of MCF-7 cells (B).

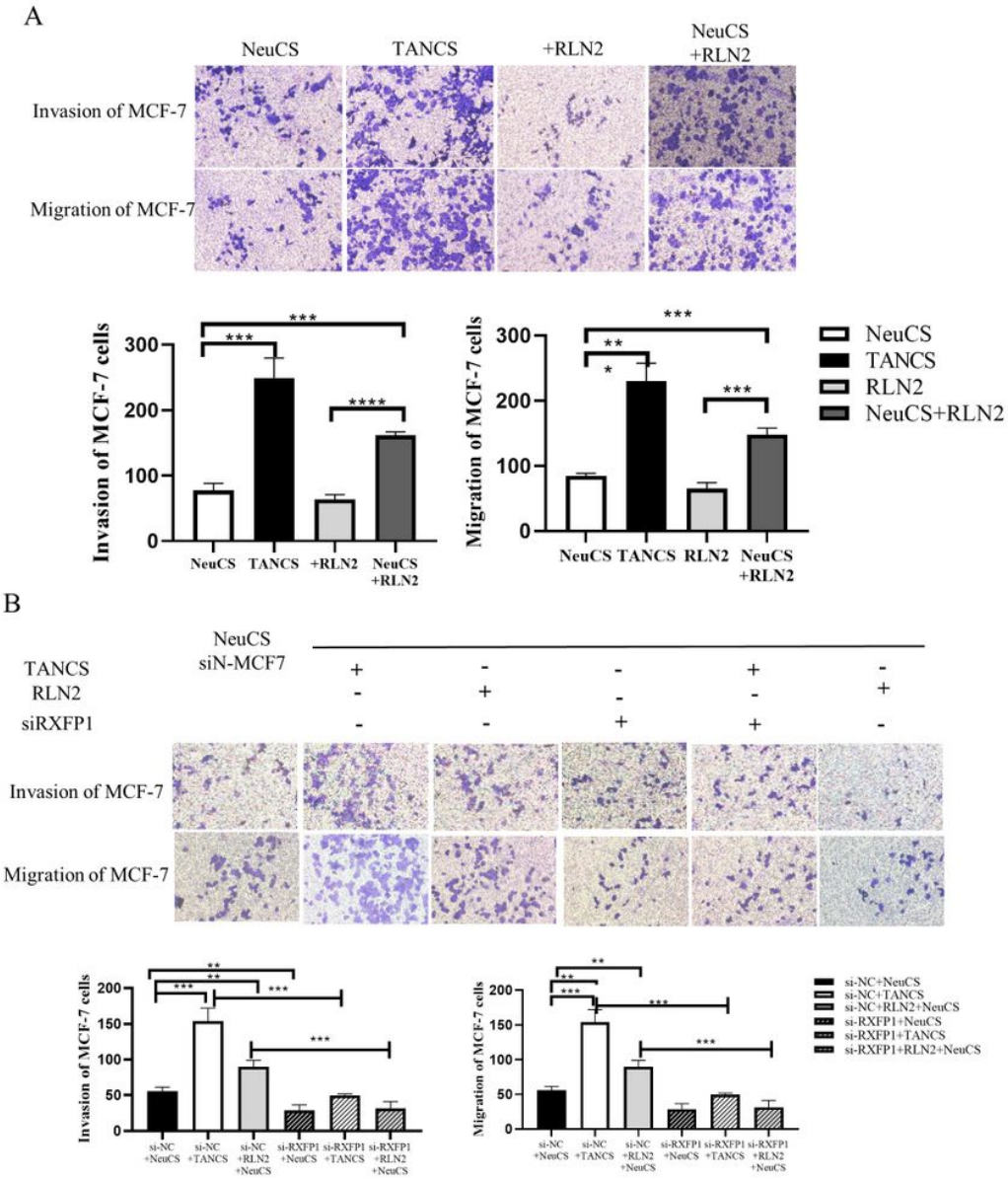

Figure 6

TANs promoted the MCF7 cells invasion and migration via RLN2-RXFP1. Invasion and migration of MCF-7 cells treated with neutrophils from MDA231CS and RLN2 (A). After treated with TANCS and NeuCS+RLN2, the invasion and migration of siRXFP1-MCF-7 cells could not be promoted (B).

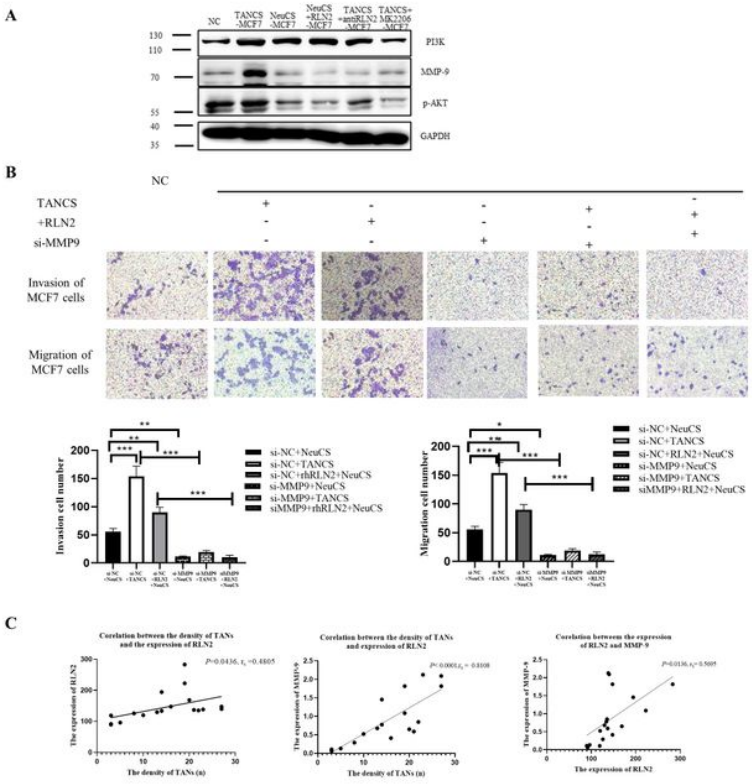

Figure 7

TANs derived RLN2 promoted MCF7 cells invasion and migration via PI3K-AKT-MMP9 axis. Western blot analysis of PI3K, p-AKT and MMP9 in siN-MCF7, TAN-siN-MCF7, Neu-siN-MCF7, Neu+RLN2-siN-MCF7 and TAN-siR-MCF7 (A). After treated with TANCS and NeuCS+RLN2, the invasion and migration of siMMP-9-MCF-7 cells could not be promoted (B). Relationship among TANs, RLN2 and MMP-9 (C) in breast cancer surgical tissues.

Supplementary Files

This is a list of supplementary files associated with this preprint. Click to download.

- FigureS1.tif
- FigureS2.tif
- FigureS3.tif
- FigureS4.tif
- FigureS5.jpg
- FigureS6.tif
- Graphicabstract.tif
- tableS1.docx
- tableS2.docx
- tableS3.docx
- uncroppedgel1.jpg

- uncroppedgel2.jpg
- uncroppedgel3.jpg
- uncroppedmembrane1.jpg
- uncroppedmembrane2.jpg
- uncroppedmembrane3.jpg